



Short communication

Electrochemical reduction of carbon dioxide: IV dependence of the Faradaic efficiency and current density on the microstructure and thickness of tin electrode

Jingjie Wu, Pranav P. Sharma, Bradley H. Harris, Xiao-Dong Zhou*

Department of Chemical Engineering, University of South Carolina, Columbia, SC 29208, United States



HIGHLIGHTS

- Sn gas diffusion electrode with 20 wt.% Nafion was optimal for the conversion of CO₂ to formate.
- The optimized Nafion fraction was found to be independent of Sn particle size (100 nm–2 μm).
- The optimized thickness of GDE was ~9 μm when 100-nm Sn particles were used with 20 wt.% Nafion.

ARTICLE INFO

Article history:

Received 29 December 2013

Received in revised form

2 February 2014

Accepted 4 February 2014

Available online 13 February 2014

Keywords:

CO₂ conversion

PEMFCs

Faradaic efficiency

Microstructure

Nafion

ABSTRACT

Central to the conversion of CO₂ in a full electrochemical cell is its cathode microstructure, which governs gas diffusion, charge exchange and transfer, and subsequently carbon dioxide reduction reaction. In this article, we report the effects of microstructure of Sn catalyst layer on the Faradaic efficiency towards formate formation as a function of Nafion loading, thickness of the catalyst layer, and catalyst particle size. Electrode with 17–20 wt.% Nafion was found to exhibit the highest partial current density towards the formation of formate when the average particle size of Sn catalysts ranged from 100 nm to 1.5 μm. This Nafion fraction is lower than what was reported, 30–36 wt.%, in the cathode of proton exchange membrane fuel cells. Moreover, the partial current density for formate formation was observed to increase with the thickness of catalyst layer, but eventually saturated because the reaction zone was limited by mass transfer. The Faradaic efficiency towards the formation of formate exhibited nearly thickness-independence due to the counteractive effects caused by increasing local proton concentration and decreasing electrical field when catalyst layer thickness was increased.

© 2014 Elsevier B.V. All rights reserved.

1. Introduction

The cathode microstructure of proton exchange membrane fuel cells (PEMFCs) plays a critical role in gas diffusion, charge exchange and transfer, and subsequently oxygen reduction reaction (ORR) as well as the overall fuel cell performance. [1,2] A generic catalyst layer in the gas diffusion electrode (GDE) consists of electrocatalyst and Nafion, [1,3,4] where Nafion allows the integration of porous catalyst layer with the electrolyte, thus increasing the three-dimensional reaction zone. The role of Nafion fraction in the catalyst layer on PEMFC performance has been reported in literature [1,4–6], which showed that the optimized Nafion fraction was in the range of 30–36 wt.%, regardless of platinum loading in the

electrodes. Recently, the configuration of PEMFCs was adopted for the electrochemical reduction of CO₂ to produce fuels [7–9]. Similar to ORR, the addition of Nafion in the catalyst layer improved the electrocatalytic activity towards CO₂ reduction by increasing the triple-phase boundary among reactant gases, electrolyte and catalyst particles. The electroreduction of CO₂, however, is expected to be more sensitive to the local proton concentration than ORR because CO₂ reduction reaction competes with hydrogen evolution reaction. As a consequence, even though this technology offers a promising approach to mitigate CO₂ in the atmosphere, it is often limited by its low Faradaic efficiency and current density, particularly towards the formation of liquid fuels [10]. Hence, it is necessary to investigate the role of cathode microstructure on the activity and selectivity of an electrochemical cell to convert CO₂ to fuels. In this article, we report our work on the effects of Nafion loading, the thickness of catalyst layer, and Sn particle size on the Faradaic efficiency and current density for the conversion of CO₂ to

* Corresponding author.

E-mail address: zhou.teaching@gmail.com (X.-D. Zhou).

formate. The electrode design was a pivotal part in our recently published research [8,11,12].

2. Experimental

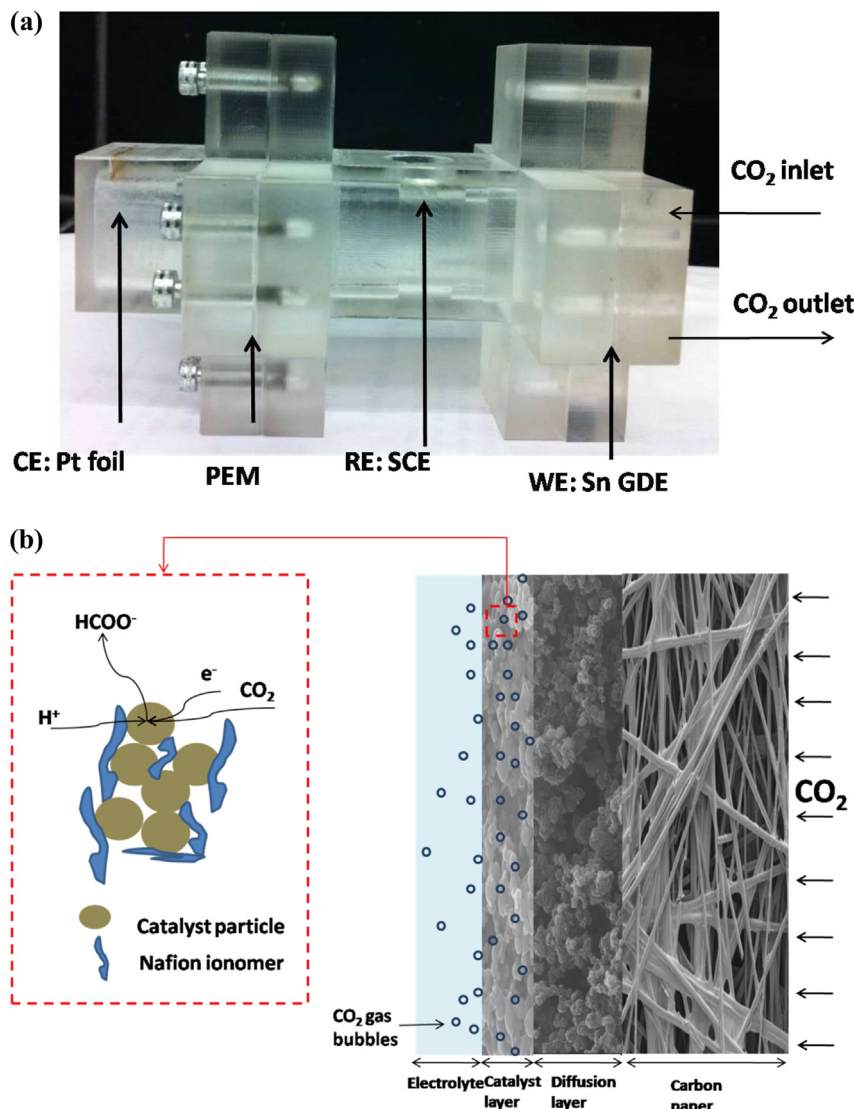
2.1. Preparation of Sn GDEs

The Sn GDE was prepared by spraying Sn catalyst ink onto a gas diffusion layer (Sigracet® GDL 10BC). The Sn catalyst ink was made by mixing Sn powders (Alfa Aesar, APS 100 nm), Nafion ionomer (DuPont), deionized water (Resistivity $\geq 18.2 \text{ M}\Omega \text{ cm}^{-2}$), and isopropanol (Sigma Aldrich), followed by ultrasonication of the mixture for an hour. In order to optimize Nafion fraction, the weight ratio of Sn:Nafion was varied from 1:1 to 20:1. In order to study the effects of Sn loading on the activity and selectivity, different Sn GDEs with loadings varying from 0.67 mg cm^{-2} to 6.55 mg cm^{-2} were also prepared with the same Nafion fraction of 20 wt.% (weight ratio Sn:Nafion of 4:1). In addition, Sn powders (Sigma Aldrich) with a size $\sim 1\text{--}2 \mu\text{m}$ were chosen to study the effect of particle size on percolation threshold and consequently electrochemical

performance of the electrode. The geometric area of Sn GDE used was 4 cm^2 .

2.2. Electrolysis

The performance of Sn GDE was evaluated in a home-made electrochemical cell (see **Scheme 1a**), in which an aqueous electrolyte, GDE, and gas CO_2 channels were assembled in series. This cell configuration enables the electrochemical reduction of CO_2 at the triple-phase interfaces as shown in **Scheme 1b**. The compartment for the working electrode was separated from that hosting the counter electrode by a proton exchange membrane (Nafion®, DuPont). The working electrode, Sn GDE, was supplied with gaseous CO_2 at 45 ml min^{-1} at 25°C and 1 atm. CO_2 flew along a serpentine channel over Sn GDEs and diffused through gas diffusion layer to Sn catalyst layer. A platinum foil ($3 \times 3 \text{ cm}^2$) and a saturated calomel electrode (SCE) were used as the counter and reference electrode, respectively. A stationary aqueous solution of 0.5 M KHCO_3 was used as the electrolyte. All the electrochemical measurements were conducted by employing Solartron 1470



Scheme 1. (a) A photo of half cell setup for measuring the electrocatalytic activity of Sn GDEs towards CO_2 reduction, and (b) schematic of CO_2 reduction at the triple-phase interfaces.

Potentiostat/Galvanostat attached to a 1255B frequency response analyzer. CO_2 electrolysis was conducted under potentiostatic conditions for 0.5 h. The linear sweep voltammetry was conducted at a scan rate of 5 mV s^{-1} . The ohmic resistance between the salt bridge tip and Sn GDE was measured by electrochemical impedance spectroscopy (EIS) with an AC perturbation of 5 mV at the open circuit condition and a logarithmic decreasing frequency sweep from 100 kHz to 0.1 Hz . All the potentials mentioned below were corrected by the iR drop unless otherwise noted. Liquid products were quantified by using $1\text{D}^1\text{H}$ nuclear magnetic resonance (NMR) spectroscopy, the details of which can be found in our previous work. [11] The charge needed to produce a specific amount of formate as determined by NMR was calculated, and divided by the total charge passed during the chronoamperometry to determine the Faradaic efficiency towards the formation of formate.

3. Results and discussion

Fig. 1a shows a cross-sectional SEM image of a Sn catalyst layer and a diffusion layer. The catalyst layer consists of 100-nm Sn nanoparticles (Sn loading = 1.56 mg cm^{-2}) and Nafion (20 wt.%). The thickness of the catalyst layer is uniform, which depends on the loading of Sn particles and Nafion. Fig. 1b shows the porous structure in the catalyst layer, comprised of agglomerates of Sn particles and the secondary pores located between these agglomerates. The structure shown in Fig. 1b is similar to that of Pt/C catalyst layer in a PEMFC [4,13]. The catalyst layers having

numerous pores are of critical importance for the liquid electrolyte and gas reactant to diffuse through for further reactions [9].

Fig. 2a shows characteristic i – V curves of three Sn GDEs without iR compensation. The Sn loading of these electrodes was maintained at 6.55 mg cm^{-2} while the Nafion fraction was $\sim 20 \text{ wt.\%}$. The i – V curves were observed not to overlap with each other because the salt bridge was placed at slightly different spots during various measurements; as a consequence, ohmic resistance between the salt bridge tip and Sn GDE was different each time (Fig. 2b). After iR correction, the three i – V curves overlapped well with each other, as shown in Fig. 2c, indicating the reproducibility of Sn GDEs. Three Sn GDEs with a lower Sn loading (1.56 mg cm^{-2}) were also measured and exhibited similar reproducibility.

The composition of the catalyst layer was varied by changing the Nafion fraction, which played a decisive role in proton transfer, CO_2 diffusion, and eventually the activity and selectivity towards CO_2 reduction. Fig. 3a shows i – V curves of the electrodes with Nafion fractions ranging from 0 to 50 wt.% but with the same Sn loading of 1.56 mg cm^{-2} . The current density increased with increasing Nafion fraction up to 20 wt.%, but then decreased, suggesting the existence of an optimized Nafion fraction to facilitate CO_2 reduction reaction. A similar trend of the Faradaic efficiency towards formate production was also observed between the potential ranging from -1.4 to -1.7 V vs. SCE (Fig. 3b). The optimized Nafion fraction for the formation of formate was $\sim 20 \text{ wt.\%}$. The electrode with this Nafion fraction exhibited a Faradaic efficiency of formate $\sim 80\%$ at -1.6 V vs. SCE. The partial current density for formate exhibited the maximum with a Nafion fraction between 17 and 20 wt.% as shown in Fig. 3c. The partial current density of formate was observed to decrease when the Nafion fraction increased to 25 wt.% or higher. This was due to the decrease of the open pore volume in Sn particles (Fig. 1b) because the excessive Nafion network blocked a fraction of open pores, which were otherwise accessible for gaseous CO_2 . It must be pointed out that electrode with 20 wt.% Nafion exhibited the optimal performance in full electrochemical cells, as reported in our recent articles [8,12].

The mechanism by which Nafion fraction influences the electrode performance is attributed to the microstructural evolution as a function of Nafion fraction. It is known that parameterizations of the properties of a catalyst layer as a function of composition refer to the class of percolation problems. In a catalyst layer comprised of Sn and Nafion, Sn particles agglomerate and form a number of pores which are filled with electrolyte, while Nafion forms a continuous frame network. To enable CO_2 reduction reaction, the pores for CO_2 diffusion, the catalyst particles for a good electronic conduction, and the Nafion matrix for proton conduction need to form a spanning network with a volume fraction above the percolation threshold [6,14]. The volume fraction for each component can be calculated based on the loading of Sn particles, the thickness of the catalyst layer, and the densities of Sn particles and Nafion ionomer [15]. The Nafion fraction of 20 wt.% corresponds to a Nafion volume fraction ~ 0.50 , hence a balance is achieved among the electronic conduction, proton conduction and CO_2 diffusion, which enables an efficient CO_2 reduction reaction. Indeed, Sn GDE with a Nafion content of 20 wt.% exhibited the highest current density and highest Faradaic efficiency of formate. The Nafion fraction in this work is lower than 30–36 wt.% as reported for PEMFC cathodes. This difference arises from two factors: (1) Pt particles (3–5 nm) used in PEMFCs are much smaller than Sn particles (100 nm–2 μm) employed in this work and (2) CO_2 reduction is more sensitive to the local proton concentration than oxygen reduction due to the presence of competition reaction of hydrogen evolution reaction with CO_2 reduction reaction. The size effect on the percolation threshold was studied by Mamunya et al.

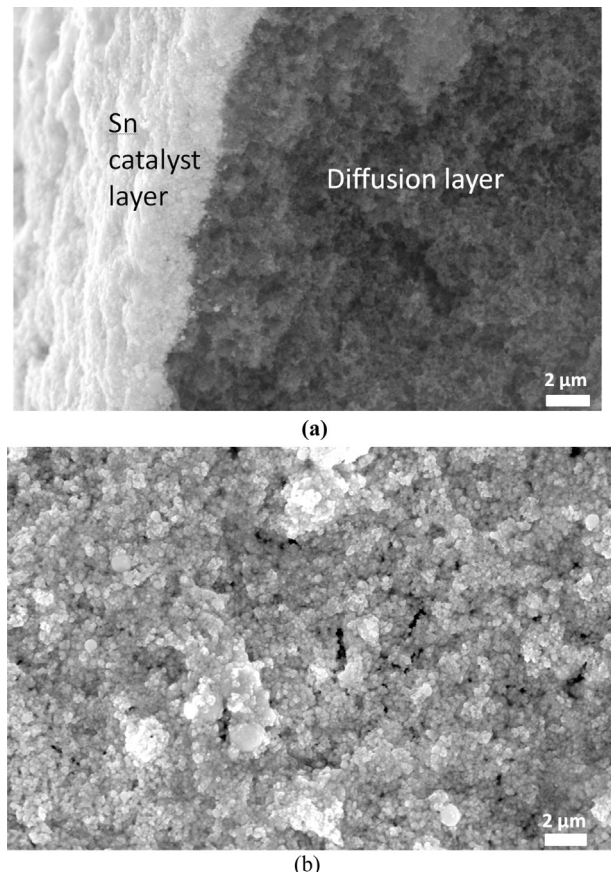


Fig. 1. SEM images of (a) the cross-section and (b) surface of Sn catalyst layer. Sn catalyst layer consists of 100 nm Sn particles with Sn loading of 1.56 mg cm^{-2} and 25 wt.% Nafion.

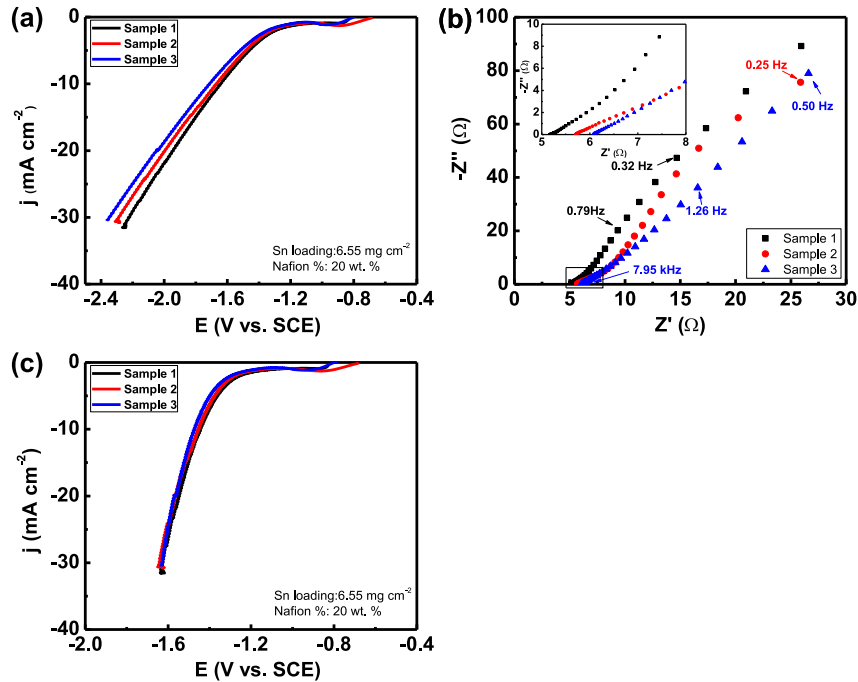


Fig. 2. (a) i – V curves of three independent Sn GDEs for CO_2 reduction before $i\text{R}$ compensation, (b) EIS measurement of ohmic resistance, (c) i – V curves after $i\text{R}$ compensation. The inset in (b) is a magnification of impedance in high frequency.

[16] on the electrical and thermal conductivity in a particulate matrix filled with an ordered shell structure. They observed that the composite having larger matrix particles (e.g. Sn particles in this research) exhibited a core–shell structure with a lower percolation threshold, which was consistent with the prediction from a universal model for percolation-threshold in a

macroscopically anisotropic material system [17,18]. In our work, when the Nafion fraction was lower than <10 wt.%, a poor performance of the electrode was observed due to the low proton conduction near the catalyst surface, and subsequently catalyst utilization was limited. While in the presence of excessive Nafion, the decrease in the electrocatalytic activity of electrode resulted

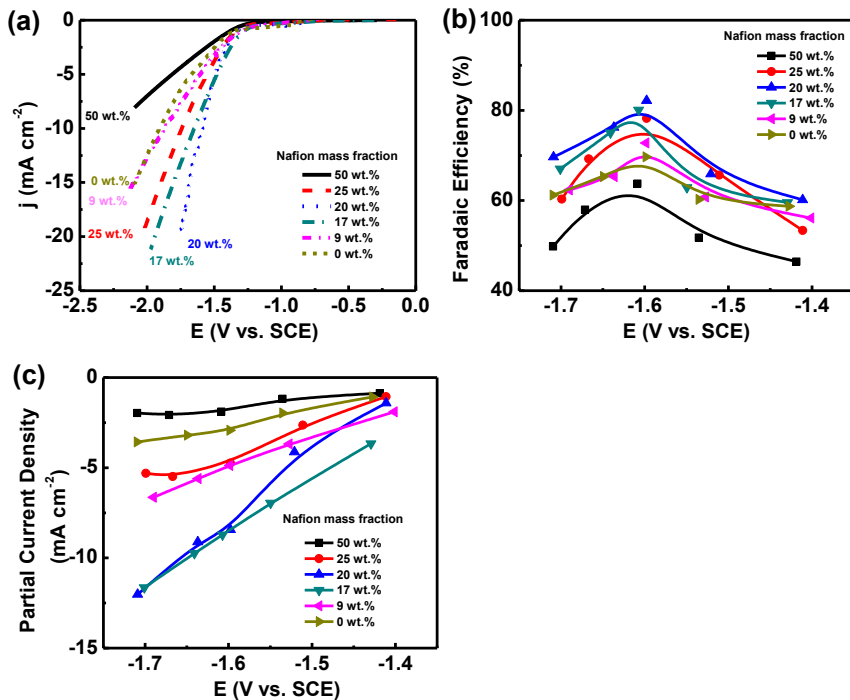


Fig. 3. Performance of Sn GDEs with various Nafion fractions and fixed Sn loading of 1.56 mg cm^{-2} . Sn GDEs consist of 100 nm Sn particles. (a) i – V characteristic curves, (b) Faradaic efficiency of formate, and (c) partial current density of formate at different potentials.

from the blockage of catalyst sites, which reduced gas permeability and increased mass transport polarization [1,5,19].

Further work was carried out to investigate the dependence of current density and Faradaic efficiency of formate on the thickness of Sn catalyst layer. The catalyst layer thickness was varied from 1.2 to 17.8 μm determined by an SEM analysis, which was equivalent to Sn loading from 0.67 to 6.55 mg cm^{-2} . The Nafion fraction was maintained at 20 wt.% for all electrodes. Figs. 4a and b show a steady increase in current density with increasing Sn loading from 0.67 to 4.00 mg cm^{-2} . The increase of current density with increasing the thickness of the catalyst layer is largely due to the increase of the total area of triple phase boundaries, at which CO_2 reduction reaction occurs. The current density started to decrease when Sn loading was $>4.00 \text{ mg cm}^{-2}$, which corresponded to a catalyst layer thickness of 9.2 μm . The decrease in current density when catalyst layer was thicker than 9.2 μm was due to the increase of diffusion resistance of the reactants [20]. This layer, $\sim 9 \mu\text{m}$, is therefore corresponding to the effective reaction zone at the cathode, including both CO_2 reduction reaction and hydrogen evolution reactions. The Faradaic efficiency towards the formation of formate was found nearly independent on the thickness of catalyst layer and was approximately 72% at -1.6 V vs. SCE (Fig. 4c). The partial current density of formate measured at -1.6 V vs. SCE was calculated from the total current density and Faradaic efficiency of formate, and then plotted as a function of Sn loading, as shown in Fig. 4c. Our previous studies showed that the Faradaic efficiency towards the formation of formate was governed by two factors: (1) the local proton concentration in the reaction zone and (2) the local electrical field [8,11]. In this work, the electrochemical cells were operated at a relatively low current density ($<30 \text{ mA cm}^{-2}$). Hence, an increase in the thickness of catalyst layer resulted in increasing current density, thus raised the local proton concentration, which was in favor of the formation of formate. At a constant applied cell potential, the increase of catalyst layer thickness and subsequently the current density, however,

contributed to a decrease in the electrical field in the catalyst layer, which impeded the formation of formate. As a consequence, when the thickness of the catalyst layer was increased, the promoting contributions from the increase of local proton concentration towards formate formation were offset by the unfavorable effects of the decrease in the local electrical field. The overall effect was that the Faradaic efficiency of formate exhibited weak thickness dependence.

Fig. 5 shows the total current density, Faradaic efficiency and partial current density of formate as a function of cathode potential and Nafion fraction with Sn particles between 1 and 2 μm used in GDEs. The highest total current density was observed in the electrode comprised of 20 wt.% Nafion (Nafion volume fraction 0.47), while the electrode with a Nafion fraction of 17 wt.% (Nafion volume fraction 0.40) showed the highest selectivity towards formate production. The electrodes consisting of 17 and 20 wt.% Nafion exhibited a similar partial current density of formate, which was higher than the electrodes with other Nafion fractions, especially at high potentials. The optimal Nafion fraction, 17–20 wt.%, for Sn GDEs consisting of $\sim 1.5 \mu\text{m}$ Sn particles was similar to that for GDEs with 100-nm Sn catalysts, suggesting Nafion exhibited in the form of polymer fragments instead of particulate clusters in catalyst layer.

4. Conclusions

The microstructure of Sn catalyst layer for CO_2 electro-reduction was systematically investigated in terms of Nafion fraction, catalyst loading, and catalyst particle size. Impregnation of electrodes with Nafion extended the three-dimensional reaction zone. This optimized microstructure provided a desirable proton concentration, electronic conduction, and gas diffusion for high selectivity towards the formation of formate. Both the current density and Faradaic efficiency towards formate formation were at the maximum with the optimized Nafion fraction of 17–20 wt.% in Sn electrodes, which

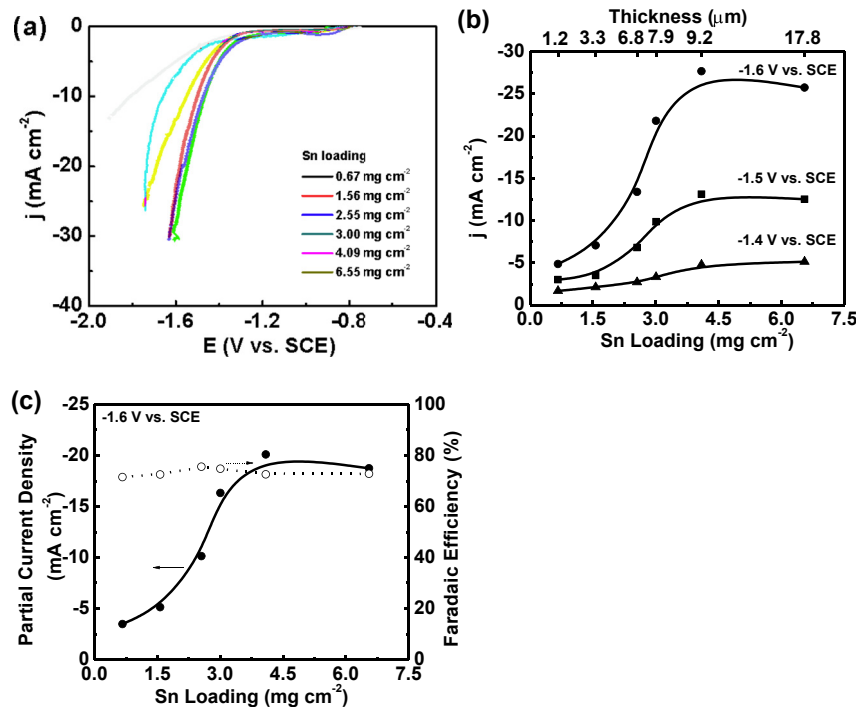


Fig. 4. Comparison of electroactivity of Sn GDEs with various Sn loadings and fixed 20 wt.% Nafion. Sn GES consists of 100 nm Sn particles. (a) i – V curves, (b) current density versus Sn loading and Sn catalyst layer thickness, and (c) Faradaic efficiency and partial current density of formate at -1.6 V vs. SCE .

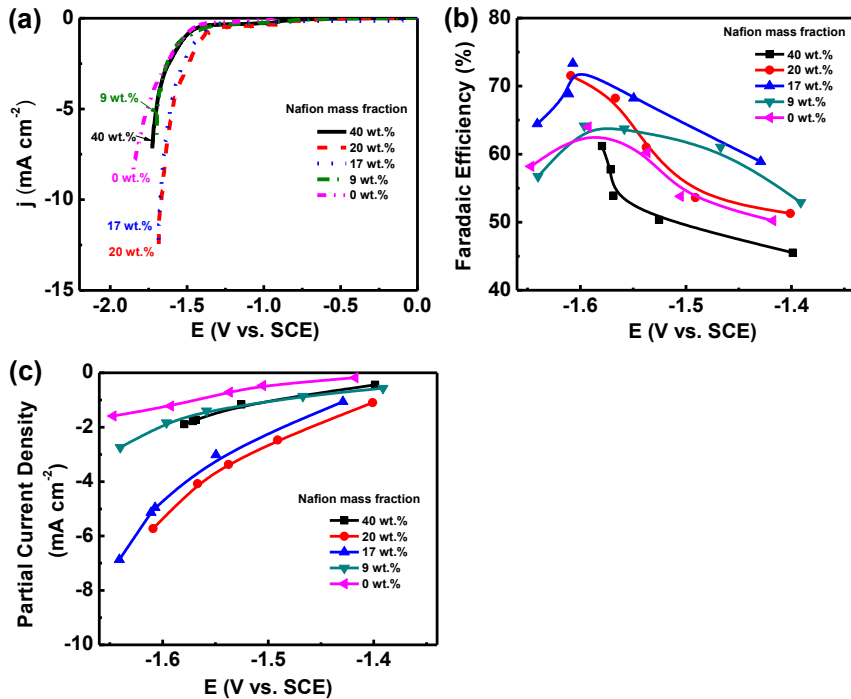


Fig. 5. Performance of Sn GDEs with various Nafion fractions and fixed Sn loading of 0.86 mg cm^{-2} . Sn GDEs consist of Sn particles with size of $1\text{--}2 \mu\text{m}$. (a) iV characteristic curves, (b) Faradaic efficiency of formate, and (c) partial current density of formate at different potentials.

was found independent on the size of catalyst particles. The current density increased with increasing Sn loading up to 4.00 mg cm^{-2} corresponding to a catalyst layer thickness of $\sim 9.2 \mu\text{m}$. Further increase of Sn loading showed a negligible contribution to the total current density, suggesting the existence of maximum reaction penetration depth.

References

- [1] E. Antolini, L. Giorgi, A. Pozio, E. Passalacqua, *J. Power Sources* 77 (1999) 136–142.
- [2] H.R. Jhong, F.R. Brushett, P.J.A. Kenis, *Adv. Energy Mater.* 3 (2013) 589–599.
- [3] S. Litster, G. McLean, *J. Power Sources* 130 (2004) 61–76.
- [4] S. Mu, M. Tian, *Electrochim. Acta* 60 (2012) 437–442.
- [5] G. Sasikumar, J.W. Ihm, H. Ryu, *Electrochim. Acta* 50 (2004) 601–605.
- [6] A. Suzuki, U. Sen, T. Hattori, R. Miura, R. Nagumo, H. Tsuibo, N. Hatakeyama, A. Endou, H. Takaba, M.C. Williams, A. Miyamoto, *Int. J. Hydrogen Energy* 36 (2011) 2221–2229.
- [7] C. Delacourt, P.L. Ridgway, J.B. Kerr, J. Newman, *J. Electrochem. Soc.* 155 (2008) B42–B49.
- [8] J. Wu, F.G. Risalvato, P.P. Sharma, P.J. Pellechia, F.-S. Ke, X.-D. Zhou, *J. Electrochem. Soc.* 160 (2013) F953–F957.
- [9] Y.G. Yoon, G.G. Park, T.H. Yang, J.N. Han, W.Y. Lee, C.S. Kim, *Int. J. Hydrogen Energy* 28 (2003) 657–662.
- [10] D.T. Whipple, P.J.A. Kenis, *J. Phys. Chem. Lett.* 1 (2010) 3451–3458.
- [11] J. Wu, F.G. Risalvato, F.-S. Ke, P.J. Pellechia, X.-D. Zhou, *J. Electrochem. Soc.* 159 (2012) F353–F359.
- [12] J. Wu, F.G. Risalvato, S. Ma, X.-D. Zhou, *J. Mater. Chem. A* 2 (2014) 1647–1651.
- [13] M. Uchida, Y. Aoyama, N. Eda, A. Ohta, *J. Electrochem. Soc.* 142 (1995) 4143–4149.
- [14] E. Passalacqua, F. Lufrano, G. Squadrato, A. Patti, L. Giorgi, *Electrochim. Acta* 46 (2001) 799–805.
- [15] Q.P. Wang, M. Eikerling, D.T. Song, Z.S. Liu, T. Navessin, Z. Xie, S. Holdcroft, *J. Electrochem. Soc.* 151 (2004) A950–A957.
- [16] Y.P. Mamunya, V.V. Davydenko, P. Pissis, E.V. Lebedev, *Eur. Polym. J.* 38 (2002) 1887–1897.
- [17] I. Balberg, *Phys. Rev. B* 31 (1985) 4053–4055.
- [18] G. Wang, *ACS Appl. Mater. Interfaces* 2 (2010) 1290–1293.
- [19] S.J. Lee, S. Mukerjee, J. McBreen, Y.W. Rho, Y.T. Kho, T.H. Lee, *Electrochim. Acta* 43 (1998) 3693–3701.
- [20] A.A. Kulikovsky, *Electrochim. Commun.* 5 (2003) 530–538.